Effect of Function-Enhanced Mesenchymal Stem Cells Infected With Decorin-Expressing Adenovirus on Hepatic Fibrosis

YOON OK JANG,[a,b] MEE-YON CHO,[c] CHAE-OK YUN,[d] SOON KOO BAIK,[a,b] KYU-SANG PARK,[e] SEUNG-KUY CHA,[e] SEI JIN CHANG,[f] MOON YOUNG KIM,[a] YOO LI LIM,[a] SANG OK KWON[a]

[a]Department of Internal Medicine, [b]Cell Therapy and Tissue Engineering Center, [c]Department of Pathology, [e]Department of Physiology, and [f]Department of Preventive Medicine and Institute of Occupational Medicine, Wonju College of Medicine, Yonsei University, Wonju, Republic of Korea; [d]Department of Bioengineering, College of Engineering, Hanyang University, Seoul, Republic of Korea

Correspondence: Soon Koo Baik, M.D., Ph.D., Division of Gastroenterology and Hepatology, Department of Internal Medicine, Wonju Severance Christian Hospital, Yonsei University, Wonju College of Medicine, 20 Ilsan-ro, Wonju, Republic of Korea. Telephone: 82-33-741-1223; E-Mail: baiksk@yonsei.ac.kr

ABSTRACT

Bone marrow-derived mesenchymal stem cells (BM-MSCs) are known to have an antifibrotic effect and could be used as vehicles for targeted gene delivery. Decorin plays a protective role against fibrogenesis by modulating the degradation of the extracellular matrix. The aim of this study was to determine whether the antifibrotic effect of a combination treatment consisting of BM-MSCs and decorin on hepatic fibrosis is superior to BM-MSCs alone. The effects of BM-MSCs infected with decorin-expressing adenovirus (DCN-MSCs) on hepatic fibrosis were examined in a rat model of thioacetamide (TAA)-induced cirrhosis. The effects of infection with decorin-expressing adenovirus and of incubation with the conditioned medium of DCN-MSCs on transforming growth factor-β (TGF-β) signaling were analyzed in immortalized human hepatic stellate cells (HSCs). According to the Laennec fibrosis scoring system, cirrhotic livers from rats treated with DCN-MSCs exhibited histological improvement compared with cirrhotic livers from rats treated with control adenovirus-infected MSCs (CA-MSCs). DCN-MSC treatment reduced hepatic collagen distribution, lowered the hydroxyproline content, and rescued liver function impairment in rats with TAA-induced cirrhosis. These protective effects were more potent with DCN-MSCs than with CA-MSCs. The upregulation of collagen-1, α-smooth muscle actin (α-SMA), TGF-β1, and Smad3 phosphorylation in cirrhotic livers was prevented by DCN-MSC administration. Intriguingly, medium from cultured DCN-MSCs blocked both Smad3 phosphorylation and exogenous TGF-β1 stimulated α-SMA synthesis in HSCs. DCN-MSCs exert strong protective effects against hepatic fibrosis by suppressing TGF-β/Smad signaling. Thus, treatment with DCN-MSCs is a potentially novel and efficient therapeutic approach for patients with intractable cirrhosis. STEM CELLS TRANSLATIONAL MEDICINE 2016;5:1247–1256

SIGNIFICANCE

A combination treatment consisting of bone marrow-derived mesenchymal stem cells (BM-MSCs) and decorin strongly inhibited the progression of thioacetamide-induced hepatic fibrosis in rats, compared with BM-MSCs alone. Furthermore, the significant inhibitory effect of BM-MSCs infected with decorin-expressing adenovirus was attributed to suppressing transforming growth factor-β (TGF-β)/Smad signaling pathway, supported by attenuation of TGF-β1 expression and inhibition of Smad3 phosphorylation. Therefore, treatment with BM-MSCs infected with decorin-expressing adenovirus could constitute a novel and efficient therapeutic approach for patients with intractable cirrhosis.

INTRODUCTION

Cirrhosis is the end stage of progressive fibrosis, which is characterized by distortion of the hepatic architecture and the formation of regenerative nodules, angiogenesis, and shunts. These symptoms eventually lead to the loss of liver function and the development of hepatocellular carcinoma [1–5]. No therapeutic modalities are available for treating advanced cirrhosis, with the exception of organ transplantation. However, organ transplantation has critical limitations that have not yet been overcome.

Recently, stem cell transplantation has been suggested as an alternative therapy for liver disease. Mesenchymal stem cells (MSCs) have many practical advantages in regenerative medicine, including their high proliferation rate, multipotent differentiation capacity, and low immunogenic properties [6, 7]. In addition, MSCs have the capacity to migrate toward sites of injury and tumor microenvironments. This unique tropism makes MSCs ideal delivery vehicles for targeted therapy. We have previously demonstrated that bone

marrow-derived mesenchymal stem cell (BM-MSC) therapy improves hepatic fibrosis in vitro, in vivo, and in clinical studies [6, 8, 9].

Decorin, a small leucine-rich proteoglycan, is a ubiquitous component of the extracellular matrix (ECM) [10–13]. Decorin binds to collagen, retards the formation of collagen fibrils, and disrupts their organization [13]. In addition, decorin blocks signaling through transforming growth factor-β (TGF-β), a key mediator of fibrogenesis, and modulates the degradation of the ECM by inducing expression of the matrix metalloproteinase collagenase-1 [14, 15]. In a human hepatic stellate cell (HSC) line, decorin has been shown to inhibit TGF-β signaling, downregulate α-smooth muscle actin (α-SMA) expression, and decrease cell proliferation [16]. These observations suggest that delivery of decorin to the liver may attenuate pathogenic fibrosis in patients with cirrhosis. Of the various gene-delivery systems available, adenoviruses have been widely used because of their ability to transfer relatively large genes. However, adenoviruses have limited utility as a targeted gene-delivery system because they rapidly disseminate into the surrounding normal tissues and maintain their biological activity for only short periods of time in vivo [17].

We hypothesized that BM-MSCs could be used as delivery vehicles for antifibrotic therapy and that this system would exhibit improved safety and efficacy compared with adenoviral gene therapy alone. We further hypothesized that BM-MSCs and decorin-expressing adenovirus may exert a synergistic effect on the recovery of liver function after fibrotic injury. In this study, we investigated the effects of BM-MSCs infected with decorin-expressing adenovirus on hepatic fibrosis in a rat model of thioacetamide (TAA)-induced cirrhosis. We also explored the mechanisms underlying their antifibrotic effects in vitro and in vivo.

MATERIALS AND METHODS

Induction of Hepatic Fibrosis in a Rat Model of Thioacetamide-Induced Cirrhosis

Seven-week-old male Sprague-Dawley rats (Orient Bio Inc., Seongnam, Korea, http://www.orient.co.kr) were maintained at room temperature (25°C) with a 12-hour/12-hour light/dark cycle. Rats were given free access to food and water throughout the 12-week experiment. Hepatic fibrosis was induced in Sprague-Dawley rats by intraperitoneal injections of TAA (Sigma-Aldrich, St. Louis, MO, http://www.sigmaaldrich.com; 300 mg per kilogram of body weight) twice a week for 12 weeks. All animal experimental procedures and protocols were approved by the Institutional Animal Care and Use Committee of Yonsei University Wonju College of Medicine.

Preparation of Decorin-Expressing Adenoviruses and Human Bone Marrow-Derived Mesenchymal Stem Cells

The preparation of decorin-expressing adenovirus (dE1-k35/lacZ/DCN) and control adenovirus (dE1-k35/lacZ) was described previously [18, 19]. Human BM-MSCs were obtained from healthy persons who voluntarily donated their bone marrow (BM) stem cells. Briefly, approximately 10–20 ml of BM was aspirated from the posterior iliac crest under local anesthesia. BM mononuclear cells were isolated through

density-gradient centrifugation (Histopaque-1077, Sigma-Aldrich). Mononuclear cells were plated (2–3 $\times$ 10^5 cells per cm^2) in a 75-cm^2 flask (Thermo Fisher Scientific Life Sciences, Waltham, MA, http://www.thermofisher.com) in Dulbecco's modified Eagle's medium (DMEM; Thermo Fisher Scientific Life Sciences) containing 10% fetal bovine serum (FBS; Thermo Fisher Scientific Life Sciences) and 1% penicillin/streptomycin (Thermo Fisher Scientific Life Sciences). Cells were cultured at 37°C in a 5% CO$_2$ atmosphere. When the cultures approached 80% confluence, the cells were harvested by treatment with trypsin/EDTA (Thermo Fisher Scientific Life Sciences) and replated in 175-cm^2 flasks at a density of 4–5 $\times$ 10^3 cells per cm^2. Cells were serially subcultured to passage four or five before injection. All procedures and protocols involving human subjects were approved by the Institutional Review Board of Yonsei University Wonju Severance Hospital (CR109021) and were conducted according to the principles of the Declaration of Helsinki. All participants provided written informed consent before study participation.

BM-MSC Immunophenotypes and Differentiation Assays

The immunophenotypes of the BM-MSCs (CD14, CD34, CD45, CD73, and CD105) were analyzed on the day of adenovirus infection, and their differentiation potentials were also determined (osteogenic and adipogenic; Fig. 1). For immunophenotyping, BM-MSCs were stained with the following antibodies conjugated to fluorescein isothiocyanate (FITC) or phycoerythrin (PE): CD14-FITC, CD34-FITC, CD45-FITC, CD73-PE, and CD105-PE (BD Biosciences, San Jose, CA, http://www.bdbiosciences.com). Briefly, 5 $\times$ 10^5 cells were resuspended in 0.2 ml of phosphate-buffered saline (PBS) and incubated with FITC- or PE-conjugated antibodies for 20 minutes at room temperature. FITC- and PE-conjugated mouse IgG isotype control antibodies were used at the same concentrations as the specific primary antibodies. The fluorescence intensities of the cells were evaluated by flow cytometry (Epics XL; Beckman Coulter, Miami, FL, https://www.beckmancoulter.com). Osteogenic differentiation was assessed by first plating the cells at 2 $\times$ 10^4 cells per cm^2 in six-well plates and then incubating them for 2–3 weeks in osteogenic medium, which consisted of DMEM supplemented with 10% FBS, 10 mM β-glycerophosphate, 10^{-7} M dexamethasone, and 0.2 mM ascorbic acid (Sigma-Aldrich) [20]. Osteogenic differentiation was assessed by quantifying the release of p-nitrophenol from p-nitrophenyl phosphate by alkaline phosphatase [21]. For adipogenic differentiation, BM-MSCs were plated at 2 $\times$ 10^4 cells per cm^2 in six-well plates and cultured for 1 week; then, differentiation was induced with adipogenic medium (10% FBS, 1 μM dexamethasone, 0.5 mM 3-isobutyl-1-methylxanthine, 10 μg/ml insulin, and 100 μM indomethacin in high-glucose DMEM) for an additional 3 weeks. The differentiated cells were fixed in 4% paraformaldehyde for 10 min, and oil droplets were stained with fresh Oil Red O solution (Sigma-Aldrich). Only MSCs that met the following criteria were used: viability greater than 80%; the absence of microbial contamination (bacteria, fungus, virus, or mycoplasma) when tested 3–4 days before administration; CD73 and CD105 expression in more than 90% of the cells; and the absence of CD14, CD34, and CD45 in less than 3% of the cells, as assessed by flow cytometry.
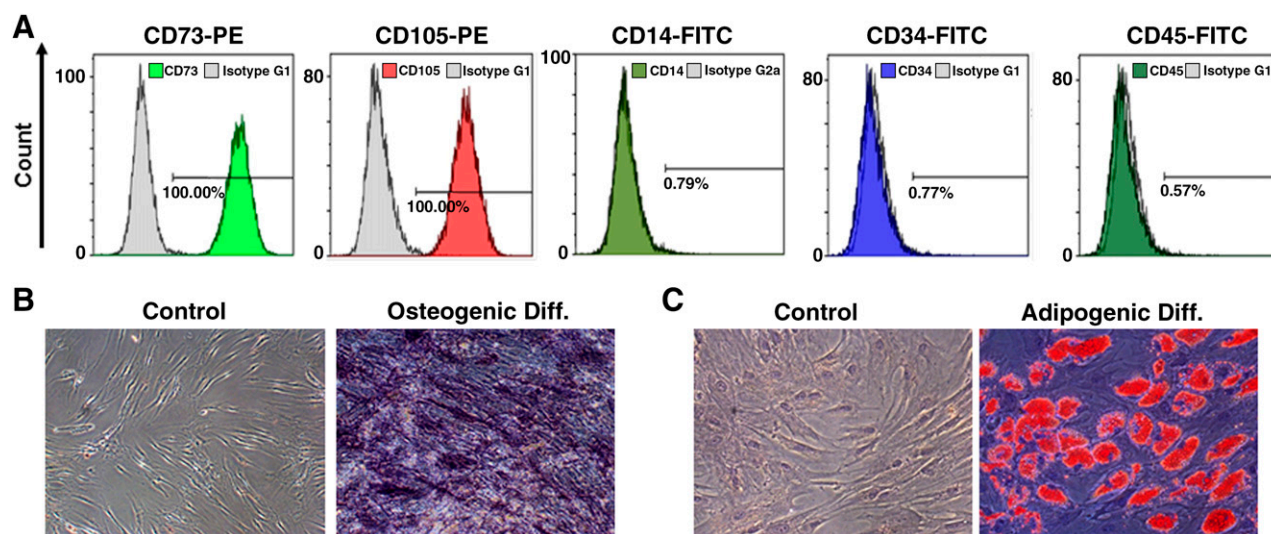
Figure 1. Immunophenotypes and differentiation potentials of bone marrow-derived mesenchymal stem cells (BM-MSCs). **(A):** Immunophenotype analysis of the BM-MSCs. The expression levels of various cell surface antigens (CD14, CD34, CD45, CD73, and CD105) were evaluated by flow cytometry. **(B):** Alkaline phosphatase staining. BM-MSCs subjected to osteogenic differentiation in osteogenic medium exhibited positive staining for endogenous alkaline phosphatase activity. In contrast, BM-MSCs incubated in control medium did not exhibit any staining (magnification: ×100). **(C):** Lipid droplet staining. BM-MSCs subjected to adipogenic differentiation in adipogenic medium exhibited positive staining for lipid droplets. In contrast, BM-MSCs incubated in control medium did not exhibit any staining (×200). Abbreviations: Diff., differentiation; FITC, fluorescein isothiocyanate; PE, phycoerythrin.

Administration of BM-MSCs Infected With Decorin-Expressing Adenovirus in a Rat Model of Thioacetamide-Induced Cirrhosis

Human BM-MSCs were infected with decorin-expressing adenovirus (dE1-k35/lacZ/DCN) or control adenovirus (dE1-k35/lacZ) at a multiplicity of infection (MOI) of 20. At 48 hours after infection, the adenovirus-infected BM-MSCs were harvested by using trypsin/EDTA.

Animals were randomly allocated into four groups (each group, $n = 18$) as follows: group I (G1, sham group); group II (G2, untreated cirrhotic group), which received the TAA injections; group III (G3, control adenovirus-infected BM-MSCs treated group), which received both the TAA injections and the control adenovirus-infected BM-MSC (CA-MSCs) treatment; and group IV (G4, decorin-expressing adenovirus-infected BM-MSC-treated group), which received both the TAA injections and the decorin-expressing adenovirus-infected BM-MSCs (DCN-MSCs) treatment. The rats were anesthetized by intramuscular administration of a mixture of Zoletil (Virbac Laboratories, Carros, France, https://www.virbac.com) and Rompun (Bayer Korea, Seoul, Korea, https://www.bayer.co.kr). By using an aseptic technique, a 1-cm incision was made caudal to the costal arch on the right flank to expose the right lobe of the liver. By using a 26-gauge needle, 1×10^6 CA-MSCs or 1×10^6 DCN-MSCs were injected directly into the right lobe of the liver at 6 and 8 weeks during the 12-week course of TAA administration (Fig. 2A). After 12 weeks, blood samples were taken, and the animals were sacrificed. Liver tissue specimens were collected, fixed, immediately frozen, and stored at −80°C for analysis.

Histomorphological and Immunohistochemical Analysis

Five-micrometer-thick sections of paraffin-embedded liver tissue were prepared and stained with hematoxylin and eosin (H&E), Masson's trichrome (MTC), and Picrosirius red. The extent of fibrosis was evaluated by using the Laennec fibrosis scoring system (supplemental online Table 1). In this system, the thickness of the predominant type of septae in each specimen is chosen, and the smallest nodule is selected for scoring. A liver pathologist who was blinded to the data evaluated the extent of fibrosis. The Laennec fibrosis scoring system was used because it incorporates three subclasses of cirrhosis, thereby enabling a more detailed estimation of the effects of the intervention on fibrosis [22]. To further assess the effects of each treatment on hepatic fibrosis, the fibrotic area in each liver sample was quantified as a percentage of the total MTC-stained area. The fibrotic area was assessed in digital photomicrographs by using a computerized image analysis system (Analysis 3.0, Olympus, Tokyo, Japan, http://www.olympus-global.com). To quantify the fibrotic area, fields of vision were selected randomly at a magnification of ×100.

Picrosirius red staining was also performed to quantify the total amount of collagen. Five-micrometer-thick sections of paraffin-embedded liver tissue were deparaffinized, rehydrated with distilled water, and stained with a Picrosirius red staining kit (Polysciences, Warrington, PA, http://www.polysciences.com) according to the manufacturer's instructions. In addition, the amount of collagen (the main component of fibrous tissue) was estimated by determining the percentage of Picrosirius red-stained area out of the total area. Collagen staining was observed on an Olympus BX51 microscope and quantified by using image analysis software (IMT i-solution, Vancouver, BC, Canada, http://www.imt-digital.com). Image artifacts and structural collagen in the large portal tracts and blood vessel walls were omitted from the total collagen area [23].

For immunofluorescence staining, frozen liver sections were fixed in cold acetone, and nonspecific binding sites were blocked by incubation in 10% bovine serum for 2 hours at room temperature. Tissue sections were then incubated with antibodies against decorin (R&D Systems, Minneapolis, MN, https://www.rndsystems.com) and monoclonal antibodies against α-SMA
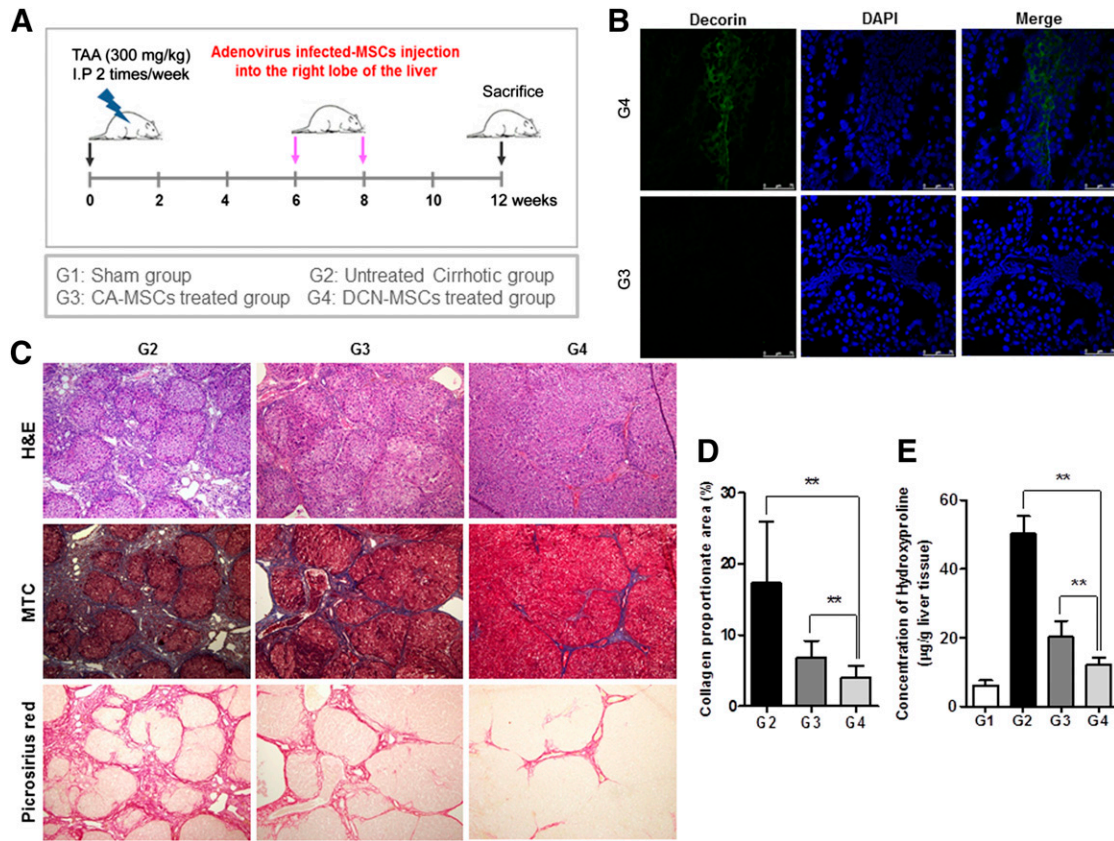
Figure 2. Treatment with bone marrow-derived MSCs infected with decorin-expressing adenovirus reverses the histological changes of hepatic fibrosis. **(A):** Experimental procedure. Hepatic fibrosis was induced in Sprague-Dawley rats by intraperitoneal injection of TAA (300 mg/kg) twice a week for 12 weeks. DCN-MSCs or CA-MSCs were injected directly into the right liver lobe at weeks 6 and 8 of the 12-week course of TAA administration. **(B):** Immunofluorescence staining of decorin in liver tissue. Decorin staining was observed on the day at which DCN-MSCs were injected into the fibrotic livers. Nuclei were stained with DAPI. Merged immunofluorescence images of decorin (green) and DAPI (blue) staining are shown. Scale bar = 75 μm. **(C):** Histological analysis was performed by H&E and MTC staining. The untreated cirrhotic group exhibited clear cirrhosis with broad septum with minute nodules (F4C). The CA-MSC-treated group exhibited cirrhosis with thin septation with rounded contours or visible large nodules (F4A), whereas the DCN-MSC-treated group showed periportal fibrosis (F2) (magnification: ×100). Picrosirius red staining of sections from liver biopsy specimens show the difference in the collagen-stained area (red) between the untreated cirrhotic group and the DCN-MSC-treated group (magnification: ×100). **(D):** Quantification of the relative Picrosirius red-stained (collagen) areas. Data were obtained by an image analysis program. **(E):** Measurement of hepatic hydroxyproline content. A colorimetric assay was used to quantify the hydroxyproline content of each liver sample. Values are expressed as means ± SDs. ∗∗, $p < .01$. Abbreviations: CA-MSCs, control adenovirus-infected mesenchymal stem cells; DAPI, 4′,6-diamidino-2-phenylindole; DCN-MSCs, decorin-expressing adenovirus-infected bone marrow-derived mesenchymal stem cells; H&E, hematoxylin & eosin; MSCs, mesenchymal stem cells; MTC, Masson's trichrome; TAA, thioacetamide.

(Abcam, Cambridge, MA, http://www.abcam.com) for 1 hour at room temperature. The slides were washed with PBS and incubated with Alexa Fluor 488 (Thermo Fisher Scientific Life Sciences)-conjugated secondary antibodies for 1 hour at room temperature in the dark. After washing, the slides were mounted with Vectashield (Vector Laboratories, Burlingame, CA, http://vectorlabs.com) mounting medium containing 4′,6-diamino-2-phenylindole (DAPI) for counterstaining of nuclei. Fluorescence images were observed on a laser scanning confocal microscope (TCS SPE, Leica Microsystems GmbH, Wetzlar, Germany, http://www2.leicabiosystems.com).

Measurement of Hepatic Hydroxyproline Content

Liver tissue was hydrolyzed with 6 N HCl for 16 hours at 120°C. The hydrolysates were then cooled, neutralized with 6 N NaOH, and spun by centrifugation at 13,000*g* for 10 minutes. The supernatants were supplemented with 7% chloramine T, acetate/citrate buffer (sodium acetate·3H$_2$O, trisodium citrate·2H$_2$O,

citric acid, and isopropanol). Ehrlich's solution (dimethylamino-benzaldehyde with perchloric acid and isopropanol) was then added, and the reactions were incubated for 35 minutes at 60°C. After cooling, the absorbance of each well was measured at 560 nm by using an Emax Precision Microplate Reader (Molecular Devices, Sunnyvale, CA, http://www.moleculardevices.com). The hydroxyproline concentration of each sample was calculated from a standard curve prepared with hydroxyproline (Sigma-Aldrich, H5534). Results are expressed as micrograms of hydroxyproline per gram of liver tissue.

Biochemical Parameter Analysis

Measurements of alanine transaminase (ALT), aspartate transaminase (AST), total bilirubin, and albumin levels were carried out by using commercially available kits (Asan Pharmaceutical, Seoul, Korea, http://www.asanpharm.com) according to the manufacturer's instructions.
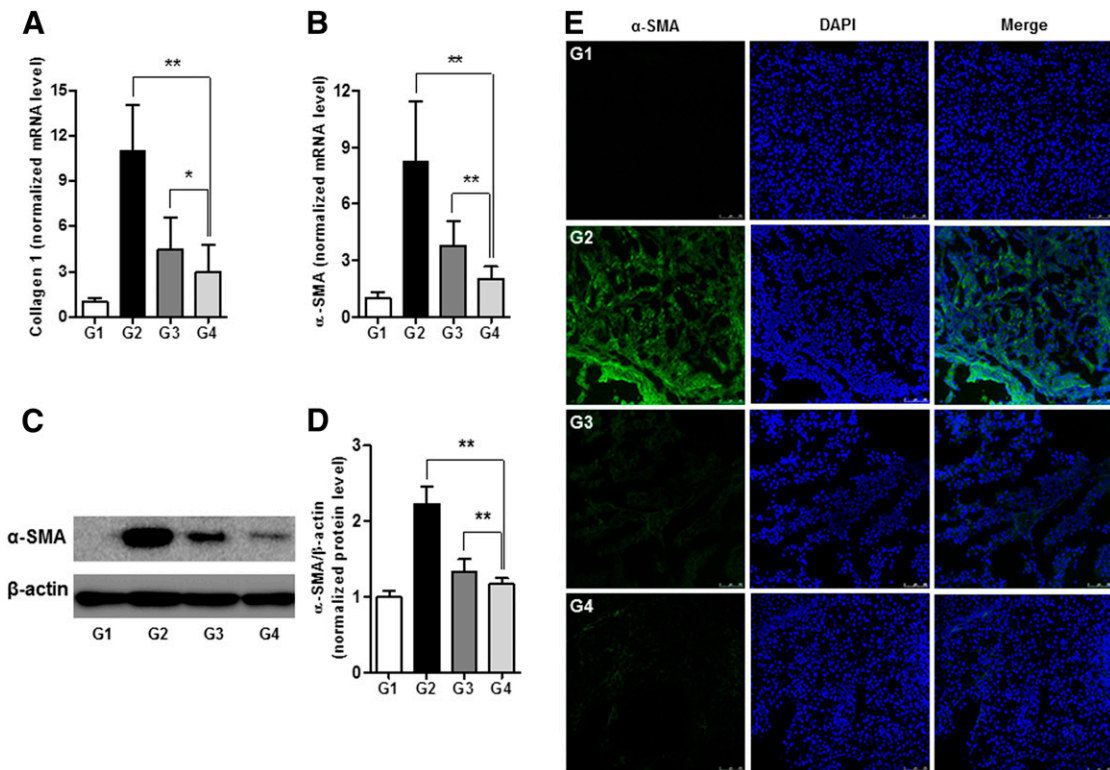
Figure 4. Bone marrow-derived mesenchymal stem cells infected with decorin-expressing adenovirus suppress hepatic fibrosis. **(A, B):** mRNA expression levels of collagen-1 **(A)** and α-SMA **(B)**. **(C, D):** Representative western blot for α-SMA **(C)** and its densitometric analysis **(D)**. Values are expressed as means $\pm$ SDs. $*$, $p < .05$, $**$, $p < .01$. **(E):** Immunofluorescence staining of α-SMA in liver tissue. The expression of α-SMA in the DCN-MSC-treated group (G4) was significantly decreased compared with the untreated cirrhotic group (G2) and the CA-MSC-treated group (G3). Nuclei were stained with DAPI. Merged immunofluorescence images of α-SMA (green) and DAPI (blue) are shown. Scale bar = 75 μm. Abbreviations: CA-MSC, control adenovirus-infected mesenchymal stem cell; DAPI, 4′,6-diamidino-2-phenylindole; DCN-MSC, decorin-expressing adenovirus-infected bone marrow-derived mesenchymal stem cell; mRNA, messenger RNA; α-SMA, α-smooth muscle actin.

Fisher Scientific Life Sciences) with DMEM (Thermo Fisher Scientific Life Sciences) containing 10% FBS (Thermo Fisher Scientific Life Sciences) and 1% penicillin/streptomycin (Thermo Fisher Scientific Life Sciences), and cultured at 37°C in a 5% CO_2 atmosphere.

Expression of α-SMA and Phospho-Smad3 in HSCs

For direct viral infection, human HSCs were plated in a 75-cm^2 flask at approximately 70% confluence and then infected with either decorin-expressing adenovirus (dE1-k35/lacZ/DCN) or control adenovirus (dE1-k35/lacZ) at an MOI of 20. At 48 hours after infection, the infected cells were treated either with or without TGF-β1 (R&D Systems). For indirect viral infection, human BM-MSCs were infected with either decorin-expressing adenovirus or control adenovirus at an MOI of 20. At 48 hours after infection, HSCs were incubated with the supernatants from virus-infected BM-MSCs for 48 hours and treated with or without TGF-β1 (R&D Systems). For the analysis of α-SMA protein levels, HSCs were treated with or without TGF-β1 (1 ng/ml) for 24 hours. For the analysis of phospho-Smad3 protein levels, HSCs were treated with or without TGF-β1 (1 ng/ml) for 30 minutes.

Statistical Analysis

All values are presented as means $\pm$ SDs. Data were analyzed by the Kruskal-Wallis H test and the Mann-Whitney test using SPSS

software version 20.0 (IBM, Armonk, NY, http://www.ibm.com). For all analyses, p values < 0.05 were considered statistically significant.

RESULTS

Validation of BM-MSCs Immunophenotypes and Differentiation Potentials

The CD14, CD34, CD45, CD73, and CD105 immunophenotypes of the cells were determined, and osteogenic or adipogenic differentiation was induced on the day of adenovirus infection (Fig. 1). CD73 and CD105 (positive markers of BM-MSCs) were expressed in more than 98% of the cells, whereas CD14, CD34, and CD45 (negative markers of BM-MSCs) were expressed in less than 1% of all cells (Fig. 1A). Therefore, the BM-MSCs had successfully differentiated into osteocytes (Fig. 1B) and adipocytes (Fig. 1C).

Treatment With BM-MSCs Infected With Decorin-Expressing Adenovirus Reverses the Histological Changes and Biochemical Parameters of Hepatic Fibrosis

Decorin expression was monitored by immunofluorescence staining after the injection of DCN-MSCs into the fibrotic rat livers. As expected, decorin was detected only in the
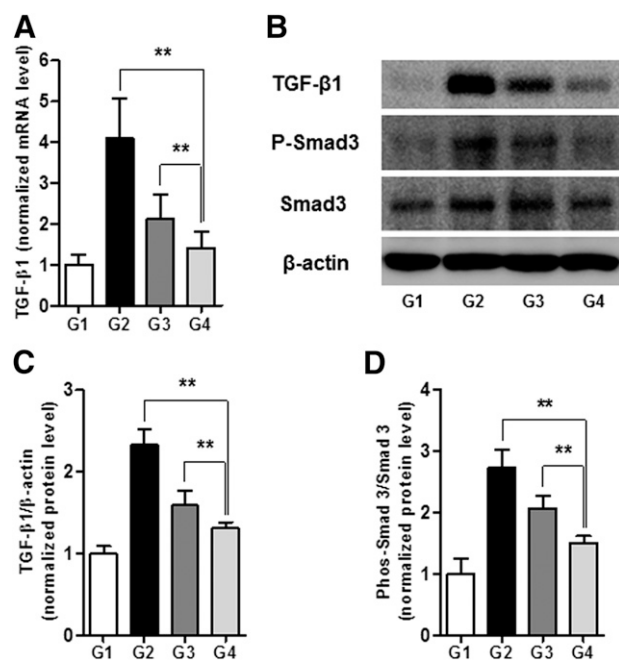
Figure 5. Bone marrow-derived mesenchymal stem cells infected with decorin-expressing adenovirus ameliorate hepatic fibrosis by inhibiting TGF-β signaling. **(A):** mRNA expression levels of TGF-β1. **(B–D):** Representative Western blot **(B)** and densitometric analysis for TGF-β1 **(C)** and phospho-Smad3 **(D)**. Values are expressed as means ± SDs. ∗∗, $p <$ .01. Abbreviation: mRNA, messenger RNA; TGF-β1, transforming growth factor-β1.

DCN-MSC-treated group, and not in the CA-MSC-treated group (Fig. 2B).

The histological changes of hepatic fibrosis were evaluated by H&E and MTC staining (Fig. 2C). The Laennec fibrosis scores revealed detailed individual changes within the cirrhotic tissue (4A–4C, supplemental online Table 1). In the untreated cirrhotic group, the liver sections exhibited strong H&E and MTC staining, revealing definite cirrhosis (stage 4 fibrosis) with regenerating nodules and fibrous septae. Treatment with CA-MSCs has been shown to elicit protective effects against fibrotic changes, a finding that is consistent with our results using autologous BM-MSCs without genetic modification [6, 8]. The CA-MSC-treated group had a significantly lower mean score compared with the untreated cirrhotic group (Table 1). The degree of fibrosis was reduced in the DCN-MSC-treated group compared with the CA-MSC-treated group, demonstrating the additional antifibrotic actions of decorin (Fig. 2C and Table 1). These results were further confirmed by Picrosirius red staining to estimate the collagen amount in each sample (Fig. 2C). The relative proportions of the Picrosirius red-stained collagen areas were determined by using image analysis software. The percentages of the collagen areas were 17.3 ± 8.65; 6.86 ± 2.35; and 3.95 ± 1.73 ($p <$ .01) in the untreated cirrhotic group (G2), the CA-MSC-treated group (G3), and the DCN-MSC-treated group (G4), respectively ($p <$ .01; Fig. 2D). The levels of hydroxyproline (μg/g) in liver tissue were 6.06 ± 1.56; 50.23 ± 5.13; 20.16 ± 4.7; and 12.03 ± 2.19 ($p <$ .01) in the sham control group (G1), G2, G3, and G4, respectively (Fig. 2E). Compared with the untreated cirrhotic group, the DCN-MSC-treated group exhibited significantly reduced collagen and lower hepatic hydroxyproline content.

The serum levels of ALT, AST, and total bilirubin were significantly increased in the TAA-induced cirrhosis group (G2) compared with G1 ($p <$ .01; Fig. 3A–3C). Treatment with DCN-MSCs (G4) markedly reduced the ALT, AST, and bilirubin levels compared with G2 ($p <$ .01). In addition, the serum level of albumin was increased in G4 compared with G2 ($p <$ .01; Fig. 3D). These changes were all greater upon treatment with DCN-MSCs compared with treatment with CA-MSCs, demonstrating the protective effects of decorin against hepatic fibrosis and liver injury.

BM-MSCs Infected With Decorin-Expressing Adenovirus Suppress Hepatic Fibrosis by Inhibiting TGF-β Signaling

The effects of decorin on the expression of collagen-1 and α-SMA in liver tissue were evaluated by quantitative real-time PCR and Western blot analysis. The relative transcript levels of collagen-1 were 1 ± 0.25; 10.95 ± 3.13; 4.44 ± 2.18; and 2.96 ± 1.84 ($p <$ .01) in G1, G2, G3, and G4, respectively (Fig. 4A). The relative mRNA levels of α-SMA were 1 ± 0.31; 8.22 ± 3.23; 3.79 ± 1.29; and 2.01 ± 0.66 ($p <$ .01), whereas the α-SMA protein levels were 1 ± 0.08; 2.23 ± 0.23; 1.33 ± 0.17; and 1.17 ± 0.08 ($p <$ .01) in G1, G2, G3, and G4, respectively (Fig. 4B–4D). The antifibrogenic effects of DCN-MSCs (G4) were consistently higher than those of CA-MSCs (G3). We also observed the expression of α-SMA in the untreated cirrhotic liver group (G2) by immunofluorescence and found that α-SMA was expressed at significantly higher levels compared with G1. However, treatment with DCN-MSCs abolished α-SMA upregulation in livers from rats with TAA-induced cirrhosis (Fig. 4E). These results suggest that adenoviral-mediated overexpression of decorin in BM-MSCs effectively prevents fibrotic changes in an animal model of cirrhosis.

We next investigated whether DCN-MSC-mediated protection against hepatic fibrosis involves TGF-β signaling. To this end, the levels of TGF-β1 expression in liver tissue from each of the groups were determined by quantitative PCR and Western blot analysis. The relative mRNA levels of TGF-β1 were 1 ± 0.25; 4.11 ± 0.95; 2.09 ± 0.59; and 1.45 ± 0.42 ($p <$ .01) in G1, G2, G3, and G4, respectively (Fig. 5A). Similarly, the relative protein levels of TGF-β1 were 1 ± 0.09; 2.33 ± 0.19; 1.59 ± 0.18; and 1.31 ± 0.07 ($p <$ .01) in G1, G2, G3, and G4, respectively (Fig. 5B, 5C). These results reveal that DCN-MSCs prevent TGF-β1 upregulation in the cirrhotic liver, which is important because TGF-β1 can act in both autocrine and paracrine manners. Furthermore, we observed that DCN-MSC treatment significantly decreased the phosphorylation of Smad3, which acts downstream of TGF-β receptor activation. The normalized levels of phosphorylated Smad3 were 1 ± 0.26; 2.74 ± 0.29; 2.07 ± 0.21; and 1.5 ± 0.12 ($p <$ .01) in G1, G2, G3, and G4, respectively (Fig. 5B, 5D). We hypothesize that decorin-expressing MSCs protect against hepatic fibrosis by efficiently blocking TGF-β mediated responses. However, it remains to be established whether the antifibrotic effect of DCN-MSCs is due to liberated decorin or another factor.

Decorin-Mediated Regulation of TGF-β1/Smad Signaling in HSCs

To investigate the mechanism by which decorin blocks TGF-β1/Smad signaling, we infected HSCs with decorin-expressing
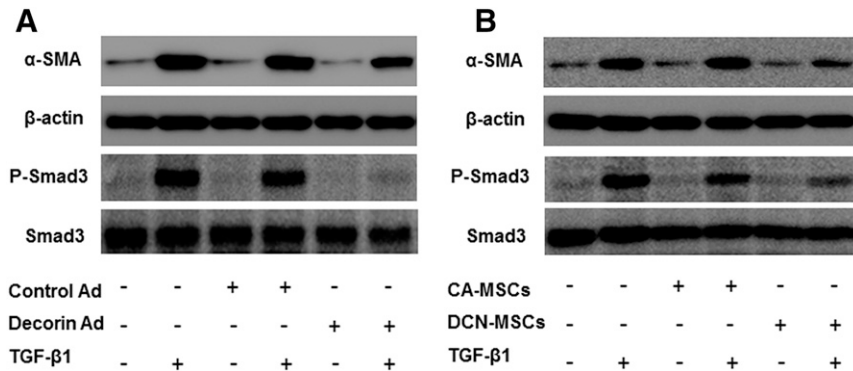
Figure 6. Effects of decorin on TGF-β/Smad signaling in HSCs. Western blot analysis of the levels of α-SMA and phospho-Smad3 in immortalized HSCs. **(A):** TGF-β1-induced changes after infection of HSCs with control adenovirus were compared with those after infection with decorin-expressing adenovirus. **(B):** Analysis of the effects of bone marrow-derived mesenchymal stem cell-conditioned medium harvested from cells infected with control adenovirus versus decorin-expressing adenovirus. Abbreviations: CA-MSCs, control adenovirus-infected mesenchymal stem cells; DCN-MSCs, decorin-expressing adenovirus-infected bone marrow-derived mesenchymal stem cells; HSCs, hepatic stellate cells; α-SMA, α-smooth muscle actin; TGF-β1, transforming growth factor-β1.

adenovirus. In parallel, we also incubated HSCs with conditioned medium from cultured DCN-MSCs. The protein levels of α-SMA and phosphorylated Smad3 in these HSCs were assessed by Western blot analysis (Fig. 6). Infection with decorin-expressing adenovirus and exposure to DCN-MSC culture medium both inhibited TGF-β1-induced upregulation of α-SMA. Moreover, phosphorylation of Smad3 by exogenous TGF-β1 was markedly reduced by adenovirus-mediated delivery of decorin into HSCs. The same effect was observed using conditioned medium from decorin-overexpressing MSCs (Fig. 6). These data indicate that the extracellular actions of liberated decorin are directly responsible for the DCN-MSC-mediated suppression of TGF-β/Smad signaling.

DISCUSSION

In this study, we found that BM-MSCs infected with decorin-expressing adenovirus exert therapeutic effects on hepatic fibrosis in a rat model of TAA-induced cirrhosis. We also investigated the mechanism by which DCN-MSC treatment ameliorates fibrotic changes. The major findings of this study are as follows: (a) direct injection of DCN-MSCs into rat livers after TAA-mediated induction of cirrhosis protected against pathogenic fibrosis; (b) DCN-MSC treatment recovered the impaired liver function in our animal model of cirrhosis; (c) DCN-MSCs inhibited TGF-β1 synthesis, Smad phosphorylation, and expression of collagen and α-SMA in the cirrhotic liver; and (d) infection of HSCs with decorin-expressing adenovirus and exposure to DCN-MSC-conditioned medium both blocked Smad phosphorylation and α-SMA upregulation by exogenous TGF-β1.

Recently, stem cell-based therapy has been proposed as a promising alternative approach for treating liver disease [24, 25]. Several studies have suggested that BM-MSCs exert therapeutic benefits in the context of hepatic fibrosis and cirrhosis [26, 27].

Decorin, a natural inhibitor of TGF-β1, is a small leucine-rich proteoglycan that binds with high affinity to TGF-β1 and prevents its interaction with profibrotic receptors. In addition, decorin regulates the production of extracellular matrix components,

inhibitors of collagen fibril maturation, and stimulators of collagenase. Therefore, the administration of decorin has been explored as a potential antifibrotic therapy in experimental kidney [28], lung [29], and human corneal fibroblast models [30]. However, the use of adenoviruses in targeted gene delivery is limited by their promiscuous native tropism, which allows the virus to infect a broad range of cells and tissues [17]. Hence, to improve the safety and efficacy of adenoviral-mediated gene therapy and identify the optimal therapeutic modality for hepatic fibrosis, efficient delivery vehicles for decorin are required.

We hypothesized that a combination treatment consisting of BM-MSCs and decorin would yield greater liver function improvement after the development of hepatic fibrosis compared with treatment with BM-MSCs alone. Through histological H&E, MTC, and Picrosirius red staining, we demonstrated that administration of decorin-overexpressing MSCs resulted in dramatic improvements in hepatic fibrosis compared with the untreated cirrhotic group. It was particularly noteworthy that DCN-MSCs exerted significantly more potent preventive effects on hepatic fibrosis compared with MSCs infected with mock adenovirus, implying that the effects of decorin and MSCs are synergistic.

In this study, we used the new Laennec fibrosis scoring system because it enables finer classification of F4 cirrhosis. This classification approach is desirable because the severity of cirrhosis exhibits clear histological variability. Furthermore, cirrhosis does not always develop in a linear manner. The development of cirrhosis can arrest or even regress over time if its root cause is removed and/or with modern antifibrotic treatment. According to the Laennec fibrosis scoring system, histological improvement from hepatic fibrosis was detected most strongly after DCN-MSC treatment ($p <$ .01). These findings were supported by immunohistochemistry, Picrosirius red staining, and hepatic hydroxyproline content analyses.

TGF-β1 has been suggested to be a key mediator for hepatic fibrosis progression [31, 32]. The fibrogenic functions of TGF-β1, such as collagen synthesis, are mediated by the canonical Smad pathway via activation of transmembrane TGF-β

receptors [1, 32]. Therefore, the TGF-β signaling pathway is considered to be an attractive therapeutic target for hepatic fibrosis treatment [1, 33, 34]. We observed significant upregulation of TGF-β1 and phosphorylated Smad3 in cirrhotic rat livers, both of which were blocked by DCN-MSC treatment. Moreover, decorin inhibited Smad3 phosphorylation in HSCs upon exogenous TGF-β1 stimulation. This finding demonstrates that decorin directly inhibits TGF-β/Smad signaling, in addition to reducing TGF-β1 release. It is intriguing that DCN-MSC-conditioned medium also blocked Smad signaling and α-SMA synthesis, both of which were observed upon overexpression of decorin in HSCs (Fig. 6). These results clearly illustrate that the liberation of decorin from DCN-MSCs contributes to their therapeutic effects against hepatic fibrosis progression.

Here we showed that administration of DCN-MSCs into the cirrhotic liver ameliorates hepatic fibrosis and that BM-MSCs and decorin act in a synergistic manner. To the best of our knowledge, this concept is completely novel. However, the clinical application of our approach is somewhat limited because the safety of adenoviruses as vectors for gene therapy has not yet been well established in humans. Further studies are necessary to determine whether our approach is clinically viable. Nevertheless, our study clearly demonstrates that DCN-MSCs exert therapeutic effects, a finding that has the potential to impact new therapeutic approaches for treating patients with intractable cirrhosis.

CONCLUSION

These findings demonstrated that combination treatment consisting of BM-MSCs and decorin strongly inhibited the progression of TAA-induced hepatic fibrosis in rats, compared with BM-MSCs alone. Therefore, treatment with BM-MSCs infected with decorin-expressing adenovirus could constitute a novel

and efficient therapeutic approach for patients with intractable cirrhosis.

AUTHOR CONTRIBUTIONS

Y.O.J.: conception and design, collection and/or assembly of data, data analysis and interpretation, manuscript writing, final approval of manuscript; M.-Y.C.: collection and/or assembly of data, data analysis and interpretation, manuscript writing, final approval of manuscript; C.-O.Y.: conception and design, provision of study material or patients, final approval of manuscript; S.K.B.: conception and design, financial support, administrative support, collection and/or assembly of data, data analysis and interpretation, manuscript writing, final approval of manuscript; K.-S.P. and S.-K.C.: data analysis and interpretation, manuscript writing, final approval of manuscript; S.J.C., M.Y.K., Y.L.L., and S.O.K.: data analysis and interpretation, final approval of manuscript.

DISCLOSURE OF POTENTIAL CONFLICTS OF INTEREST

The authors indicated no potential conflicts of interest.

REFERENCES

1 Friedman SL. Mechanisms of hepatic fibrogenesis. Gastroenterology 2008;134:1655–1669.
2 Friedman SL. Liver fibrosis—from bench to bedside. J Hepatol 2003;38(suppl 1):S38–S53.
3 Bolondi L, Gramantieri L. From liver cirrhosis to HCC. Intern Emerg Med 2011;6(suppl 1): 93–98.
4 Kim MY, Baik SK, Yea CJ et al. Hepatic venous pressure gradient can predict the development of hepatocellular carcinoma and hyponatremia in decompensated alcoholic cirrhosis. Eur J Gastroenterol Hepatol 2009;21:1241–1246.
5 Kim G, Cho YZ, Baik SK. Assessment for risk of bias in systematic reviews and meta-analyses in the field of hepatology. Gut Liver 2015;9: 701–706.
6 Jang YO, Kim MY, Cho MY et al. Effect of bone marrow-derived mesenchymal stem cells on hepatic fibrosis in a thioacetamide-induced cirrhotic rat model. BMC Gastroenterol 2014; 14:198.
7 Eom YW, Shim KY, Baik SK. Mesenchymal stem cell therapy for liver fibrosis. Korean J Intern Med 2015;30:580–589.
8 Jang YO, Kim YJ, Baik SK et al. Histological improvement following administration of

autologous bone marrow-derived mesenchymal stem cells for alcoholic cirrhosis: A pilot study. Liver Int 2014;34:33–41.
9 Jang YO, Jun BG, Baik SK et al. Inhibition of hepatic stellate cells by bone marrow-derived mesenchymal stem cells in hepatic fibrosis. Clin Mol Hepatol 2015;21:141–149.
10 Iozzo RV. The biology of the small leucine-rich proteoglycans. Functional network of interactive proteins. J Biol Chem 1999;274: 18843–18846.
11 Ameye L, Young MF. Mice deficient in small leucine-rich proteoglycans: Novel in vivo models for osteoporosis, osteoarthritis, Ehlers-Danlos syndrome, muscular dystrophy, and corneal diseases. Glycobiology 2002;12:107R–116R.
12 Schaefer L, Iozzo RV. Biological functions of the small leucine-rich proteoglycans: From genetics to signal transduction. J Biol Chem 2008;283:21305–21309.
13 Yamaguchi Y, Mann DM, Ruoslahti E. Negative regulation of transforming growth factor-beta by the proteoglycan decorin. Nature 1990;346:281–284.
14 Vogel KG, Paulsson M, Heinegård D. Specific inhibition of type I and type II collagen fibrillogenesis by the small proteoglycan of tendon. Biochem J 1984;223:587–597.

15 Danielson KG, Baribault H, Holmes DF et al. Targeted disruption of decorin leads to abnormal collagen fibril morphology and skin fragility. J Cell Biol 1997;136:729–743.
16 Shi YF, Zhang Q, Cheung PY et al. Effects of rhDecorin on TGF-beta1 induced human hepatic stellate cells LX-2 activation. Biochim Biophys Acta 2006;1760:1587–1595.
17 Coughlan L, Alba R, Parker AL et al. Tropism-modification strategies for targeted gene delivery using adenoviral vectors. Viruses 2010;2:2290–2355.
18 Choi IK, Lee YS, Yoo JY et al. Effect of decorin on overcoming the extracellular matrix barrier for oncolytic virotherapy. Gene Ther 2010;17:190–201.
19 Lee WJ, Ahn HM, Roh H et al. Decorin-expressing adenovirus decreases collagen synthesis and upregulates MMP expression in keloid fibroblasts and keloid spheroids. Exp Dermatol 2015;24:591–597.
20 Hu Y, Liao L, Wang Q et al. Isolation and identification of mesenchymal stem cells from human fetal pancreas. J Lab Clin Med 2003; 141:342–349.
21 Martin JY, Dean DD, Cochran DL et al. Proliferation, differentiation, and protein synthesis of human osteoblast-like cells (MG63)

cultured on previously used titanium surfaces. Clin Oral Implants Res 1996;7:27–37.

22 Kim MY, Cho MY, Baik SK et al. Histological subclassification of cirrhosis using the Laennec fibrosis scoring system correlates with clinical stage and grade of portal hypertension. J Hepatol 2011;55:1004–1009.

23 Calvaruso V, Burroughs AK, Standish R et al. Computer-assisted image analysis of liver collagen: Relationship to Ishak scoring and hepatic venous pressure gradient. Hepatology 2009;49:1236–1244.

24 Duncan AW, Dorrell C, Grompe M. Stem cells and liver regeneration. Gastroenterology 2009;137:466–481.

25 Kim G, Eom YW, Baik SK et al. Therapeutic effects of mesenchymal stem cells for patients with chronic liver diseases: Systematic review and meta-analysis. J Korean Med Sci 2015;30: 1405–1415.

26 Terai S, Ishikawa T, Omori K et al. Improved liver function in patients with liver cirrhosis after autologous bone marrow cell infusion therapy. STEM CELLS 2006;24: 2292–2298.

27 Kharaziha P, Hellström PM, Noorinayer B et al. Improvement of liver function in liver cirrhosis patients after autologous mesenchymal stem cell injection: A phase I-II clinical trial. Eur J Gastroenterol Hepatol 2009;21: 1199–1205.

28 Border WA, Noble NA, Yamamoto T et al. Natural inhibitor of transforming growth factor-beta protects against scarring in experimental kidney disease. Nature 1992;360: 361–364.

29 Giri SN, Hyde DM, Braun RK et al. Antifibrotic effect of decorin in a bleomycin hamster model of lung fibrosis. Biochem Pharmacol 1997;54:1205–1216.

30 Mohan RR, Gupta R, Mehan MK et al. Decorin transfection suppresses profibrogenic genes and myofibroblast formation in human corneal fibroblasts. Exp Eye Res 2010;91: 238–245.

31 Gressner AM, Weiskirchen R. Modern pathogenetic concepts of liver fibrosis suggest stellate cells and TGF-beta as major players and therapeutic targets. J Cell Mol Med 2006; 10:76–99.

32 Dooley S, ten Dijke P. TGF-β in progression of liver disease. Cell Tissue Res 2012;347: 245–256.

33 Inagaki Y, Higashiyama R, Higashi K. Novel anti-fibrotic modalities for liver fibrosis: Molecular targeting and regenerative medicine in fibrosis therapy. J Gastroenterol Hepatol 2012;27(suppl 2):85–88.

34 Rosenbloom J, Mendoza FA, Jimenez SA. Strategies for anti-fibrotic therapies. Biochim Biophys Acta 2013;1832:1088–1103.

See www.StemCellsTM.com for supporting information available online.